

Geophysical Research Letters

RESEARCH LETTER

10.1029/2021GL094129

Key Points:

- Blocking frequency is often underestimated in climate models, including in the Community Atmosphere Model
- Improving the moist parametrization by switching to a super-parametrized version increases the root-mean-square error versus reanalysis
- Correcting the bias in model mean state improves blocking frequency estimates, decreasing the error versus reanalysis from 0.015 to 0.011

Supporting Information:

Supporting Information may be found in the online version of this article.

Correspondence to:

N. Kleiner,
ekleiner@harvard.edu






Citation:

Kleiner, N., Chan, P. W., Wang, L., Ma, D., & Kuang, Z. (2021). Effects of climate model mean-state bias on blocking underestimation. *Geophysical Research Letters*, 48, e2021GL094129. <https://doi.org/10.1029/2021GL094129>

Received 28 APR 2021

Accepted 16 JUN 2021

Effects of Climate Model Mean-State Bias on Blocking Underestimation

Ned Kleiner¹ , Pak Wah Chan^{1,2} , Lei Wang^{1,3} , Ding Ma¹ , and Zhiming Kuang^{1,4} 

¹Department of Earth and Planetary Sciences, Harvard University, Cambridge, MA, USA, ²Currently at College of Engineering, Mathematics and Physical Sciences, University of Exeter, Exeter, UK, ³Currently at Department of Earth, Atmospheric, and Planetary Sciences, Purdue University, West Lafayette, IND, USA, ⁴John A. Paulson School of Engineering and Applied Sciences, Harvard University, Cambridge, MA, USA

Abstract In discussions of extreme weather trends, the subject of atmospheric blocking remains an open question, in part because of the inability of climate models to accurately reproduce blocking frequency patterns for the current climate. A number of factors have been proposed to explain this failure, including specific problems with model physics and inadequate resolution. In this paper, we show that, in the case of the National Center for Atmospheric Research Community Atmosphere Model (NCAR CAM), its underestimation of blocking frequency is caused by its mean state bias and that correcting that bias increases blocking frequency estimates over Europe and decreases the root-mean-square error versus reanalysis from 0.015 to 0.011.

Plain Language Summary Atmospheric blocking events are long-lasting weather formations that can cause destructive droughts, heat waves, or flooding. However, they are often underestimated in leading climate models, which means that predictions about how common blocking will be in a changing climate are unreliable. We applied an algorithm to the model that caused it to more closely resemble the observed climate and saw improved blocking estimates, suggesting that the cause of this underestimation is the failure of the model to precisely reproduce the climatological mean state of the real atmosphere, and that improvements in blocking estimates will come from eliminating these biases in the model. With better estimates, we will be better able to predict how the frequency of blocks—and the extreme weather that accompanies them—will change in the future.

1. Introduction

Atmospheric blocking occurs when pressure systems remain quasi-stationary in the midlatitudes for days to weeks (Rex, 1950). These “blocks” can have a major impact on surface conditions, often leading to persistent temperature extremes that can have devastating effects on human health and activities (e.g., Pfahl & Wernli, 2012). As a result, predictions of how extreme weather patterns might shift due to climate change will need to incorporate changes in blocking frequency (or lack thereof) (Chan et al., 2019).

However, current climate models do a poor job of reproducing observed blocking patterns in the current climate (Masato et al., 2013), a result that has likely contributed to the disagreement in the literature over future trends (Francis & Vavrus, 2012; Kennedy et al., 2016; Woollings et al., 2018). In line with previous results, we find substantial underestimation of blocking in an atmosphere-only run of the Community Earth Systems Model (CESM) compared to reanalysis data from the Modern Era Retrospective-Analysis for Research and Applications, Version 2 (MERRA) (Gelaro et al., 2017), as measured using the absolute geopotential height (AGP) index from Scherrer et al. (2006) (as shown later in Figure 4).

In this letter, we focus on determining what aspect of the model is at the root of this underestimation. A number of studies have pointed to various fixes that might improve blocking estimations—higher resolution (Schiemann et al., 2017), better orography (Berckmans et al., 2013), more realistic sea surface temperatures (Scaife et al., 2011), and others—without determining precisely what physical mechanism caused the better estimations. By changing the model on a more basic level, we hope to determine the root cause of blocking underestimation and thereby help guide future efforts to improve these estimations. It has not previously been known whether model biases affect blocking directly or whether they simply indirectly influence it through degradation of the model mean state. In this study, we improve the model moist physics and the

model mean state and find that the former change has little effect on blocking statistics while the latter improves them substantially. This suggests that an improved representation of diabatic heating (which we expect to see in a super-parametrized model) is not sufficient to improve the model's blocking estimations because it fails to improve the model's mean state.

2. Methods

2.1. Blocking Index

The Scherrer et al. (2006) index is a 2-dimensional index that extends the Tibaldi and Molteni (1990) index by searching for blocks across a range of central latitudes. The index uses only the 500-hPa geopotential height, and looks at grid points between 35°N and 75°N. The blocking index consists of two criteria, which are applied to each grid point:

1. The 500 hPa geopotential height is lower 15° to the South, indicating a jet reversal.
2. The 500 hPa geopotential height is more than 150m lower 15° to the North, indicating an excursion of the jet around the blocked area.

To qualify as a block, conditions at a grid point must meet these criteria for at least five consecutive days.

To confirm that the improvements we saw were not a result of our choice of blocking index, we also track events with high local wave activity (LWA), following Martineau et al. (2017). This method follows regions of very high LWA, and counts them as blocks only if they are approximately stationary for five or more days.

We also use an anomaly based index, which gives results that are less conclusive than the Scherrer et al. (2006) or Martineau et al. (2017) indices. For this index, a block at a given gridpoint consists of five or more days with 500 hPa geopotential height that is more than 250 m higher than the mean at that point.

2.2. CAM

We use the Community Atmospheric Model, Version 4 (CAM), which is the atmospheric portion of CESM, from the National Center for Atmospheric Research. We run it at a resolution of 2.5° longitude by 1.9° latitude, with 26 model levels, and a 30-min time step. We use climatological sea surface temperatures with fixed present-day levels of greenhouse gases. For the control run, we run it for 39 years and use only the January data.

In order to allow us to more easily perform a mean-state bias correction (see Section 2.4), we also modify CAM such that it is able to run in a “perpetual” January, with variables like sea surface temperature, zenith angle, and ice cover all fixed at the appropriate levels for Mid-January. We then run an ensemble where this perpetual January is the only modification from the control CAM; those results have broadly similar mean state and blocking patterns to the control run when measured using the Scherrer et al. (2006) index (see Figures S3 and S4). Mid-January is chosen because it is the time when blocking frequency is at its highest in the Northern Hemisphere (Tyrlis & Hoskins, 2008). In order to maintain a level footing between the different sources of data, even though the perpetual January is running continuously we cut its output into “months” of 31 days and reset the blocking index at the beginning of each of these months so that the frequency of blocks in perpetual CAM is not artificially inflated due to the duration criterion.

2.3. Super-Parametrized CAM (SPCAM)

The physics of a climate model include many parametrizations, problems with any one of which could, in theory, be responsible for the underestimation of blocks. In particular, the parametrization that seems to cause the greatest difference between model results and observations is the convective parametrization, which is blamed for a number of persistent model problems: the double Inter-Tropical Convergence Zone (Bellucci et al., 2010), too-low intraseasonal variability (Maloney & Hartmann, 2001), and a precipitation amount distribution that is skewed toward drizzle (Wang et al., 2016). As a result, one of the most effective ways to “improve” the model physics is to do away with the convective parametrization by resolving clouds.

Opinions differ on the importance of moist processes for atmospheric blocking (Nakamura & Huang, 2018; Pfahl et al., 2015), but it is certainly plausible that a lack of strong storms might be related to the blocking underestimation, since several prominent theories suggest that blocks are sustained by eddies that are frequently spun up in the Atlantic and Pacific storm tracks (Shutts, 1983; Yamazaki & Itoh, 2009). In particular, given the demonstrated impact of latent heat release in cyclones approaching a block (Steinfeld & Pfahl, 2019), it is conceivable (though, as we show, incorrect in this case) that an improvement in the model's representation of diabatic processes would improve the blocking frequency regardless of its effects on the model mean state.

In order to “improve” the moist physics, we compared runs of CAM with the Super-Parametrized CAM, which replaces conventional convection parametrization with a two-dimensional cloud-resolving model in each of the CAM vertical columns (Khairoutdinov et al., 2005). SPCAM has been shown to improve the performance of the model in more accurately reproducing observed precipitation patterns, including peak precipitation time within the diurnal cycle, percentage of days with significant precipitation, and convective intraseasonal variation (Khairoutdinov et al., 2005). This comparison allows us to directly test how much impact biases in the moist physics have on blocking frequency.

2.4. Mean State Bias Correction

It is, of course, more difficult to simply “improve” the mean state of the model in a way that does not risk contaminating the dynamics of blocking. Previous work has used a method of bias correction that is performed after the model is run, by adding or subtracting an array of time-invariant values from the output geopotential height so that the model mean state matches the reanalysis at each grid point (Scaife et al., 2011; Simpson et al., 2020), as well as in some cases by adjusting the high- and low-frequency variability (Vial & Osborn, 2012). This approach has had promising results but does run the risk of creating “synthetic” blocks in the output that did not behave like blocks while the model was running—while the dynamical mechanism that maintains blocks is not entirely understood, we know that there is such a mechanism from the fact that blocks are distinguishable from red noise (Masato et al., 2009), and these “synthetic” blocks might not be sustained by the same forces. For this study, we instead design an algorithm, similar to the one used in Ma and Kuang (2016), to nudge the mean state of the model while it is running without influencing the formation of the blocks directly by damping only the lowest frequencies that have little to no influence on synoptic phenomena.

To do this, we begin with the perpetual January setup in order to avoid the effects of a seasonal cycle. We begin with 38 January 15ths from the MERRA-2 reanalysis, each of which is run through CAM for 24 h to damp out artificial fluctuations; the outputs of those runs are then averaged together. This average day, or more precisely the eight three-hour intervals that make up the average day, is used as a target state (or states) for the nudging. Each ensemble member begins from a different January 15th in the MERRA database (38 ensemble members in total); then as the model runs, we track the running average of the difference between each ensemble member and the target state at each gridpoint for four variables: Zonal and meridional wind, temperature, and humidity. This “average” difference is used to determine the nudging strength and direction at each point: for example, if a point has been consistently hotter than the target, then an amount of static energy proportional to the average temperature difference is removed from that gridbox. When the ensemble begins, the nudging force adapts very quickly, since the running mean is initially drawn from only a short time period—on the second day the running mean is drawn entirely from the first day but after that each day is incorporated into the mean with a weight that is proportional to the inverse of the time elapsed. Over time, we decrease the weights to make the nudging force less adaptive until eventually (after 1,000 days) we let the weighting stay at a constant value such that each new 30-min timestep changes the running mean by only 1/24,000. The weight w_t at a given timestep t is given by the equations:

$$w_t = \frac{2}{1+t}, t < 48000 \quad (1)$$

$$w_t = \frac{1}{24000}, t \geq 48000 \quad (2)$$

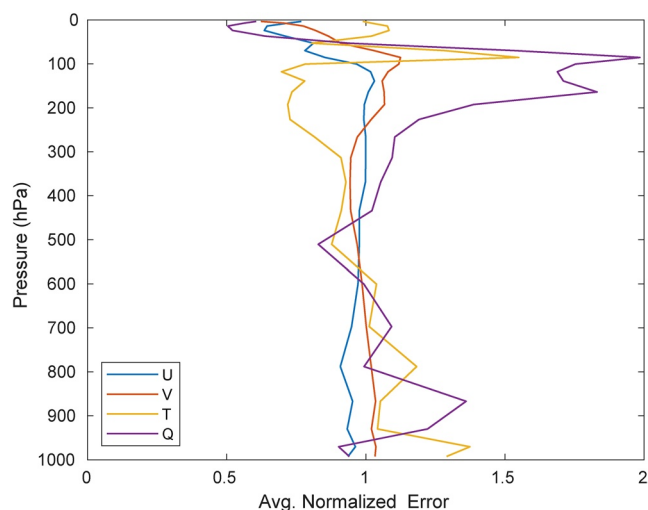


Figure 1. The magnitude of the error between the January mean states of super-parametrized Community Atmosphere Model (SPCAM) and Modern Era Retrospective-Analysis for Research and Applications, Version 2 (MERRA), normalized by the magnitude of the error between the January mean states of the control run and MERRA, for each of the four variables, calculated by finding $|X_{\text{SPCAM}} - X_{\text{MERRA}}|$ and $|X_{\text{CTL}} - X_{\text{MERRA}}|$ at each gridpoint, where X represents the average value of a variable over all timesteps, and averaging those quantities horizontally before dividing the former value by the latter.

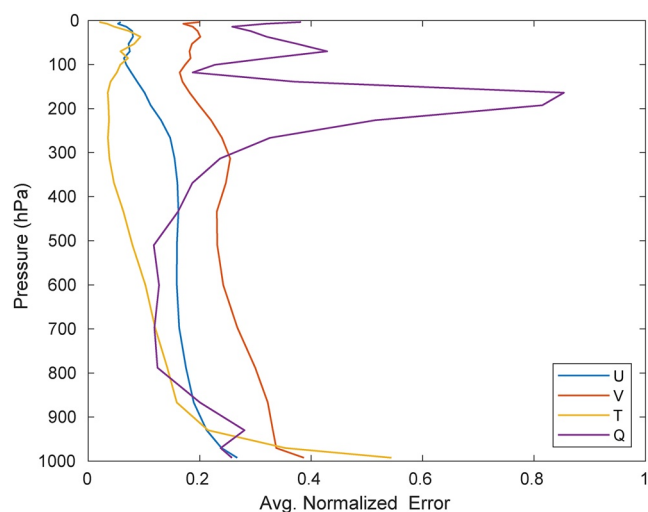


Figure 2. The magnitude of the error between the mean state of the nudged run and the January mean state of Modern Era Retrospective-Analysis for Research and Applications, Version 2 (MERRA), normalized by the magnitude of the error between the January mean states of the control run and MERRA, for each of the four nudged variables calculated in a similar manner as Figure 1.

The effective damping timescale of this nudging for oscillations of various periods is shown in Figure S5 (see the caption of which for more details on the calculation method). The “crossing point” on that plot is 56 days, meaning that oscillations shorter than that length should not be damped effectively because they will have already undergone one full period by the time they would experience substantial damping. This is more than twice the length of the vast majority of blocking events (Tyrllis & Hoskins, 2008), reassuring us that the nudging should not affect blocking frequency directly.

To demonstrate that it is the improvement in the mean state and not merely the implementation of the nudging mechanism that is responsible for the blocking frequency improvement, we do an additional nudged run, this time targeted for the mean January of the control run rather than the MERRA January mean. This run does not produce any significant change relative to the control run according to the Scherrer or Martineau blocking indices (see Figure S6).

Each ensemble member is run for 12 years; we draw our blocking statistics and climatology from only the last two years to be confident that the ensemble has reached an equilibrium between the nudging toward the target state and the drift away from it.

2.5. Significance

The statistical significance of the difference in blocking frequencies (between MERRA and model results) is evaluated using a 2-sided Student’s t test applied at each grid point, where the null hypothesis is that the model blocking frequency is identical to reanalysis.

3. Results

3.1. SPCAM

In our run of SPCAM (which lasted only 20 years because of its high computational expense) we find that the blocking frequency patterns in SPCAM are fairly similar to those in the control (Figure 4): the root-mean-square error (RMSE) between SPCAM and MERRA is 0.022, worse than between the control run and MERRA. This change is primarily the result of overprediction of low-latitude blocks, which are more related to subtropical highs than to the jet stream, but the overall result demonstrates that the parametrization of moist processes does not have a substantial impact on blocking frequency at higher latitudes. Moreover, since SPCAM does no better than CAM at matching the MERRA mean state (see Figure 1), this result supports the idea that the mean state bias is the most important factor.

3.2. Nudged CAM

The bias correction is successful at eliminating more than 50% of the error relative to the control run at almost all model levels (Figure 2). For temperature and zonal wind, we correct more than 70% of the error at all but the lowest levels, which are hard to correct likely because of noise caused by fluxes from the land surface and damping caused by the use of climatological sea surface temperatures.

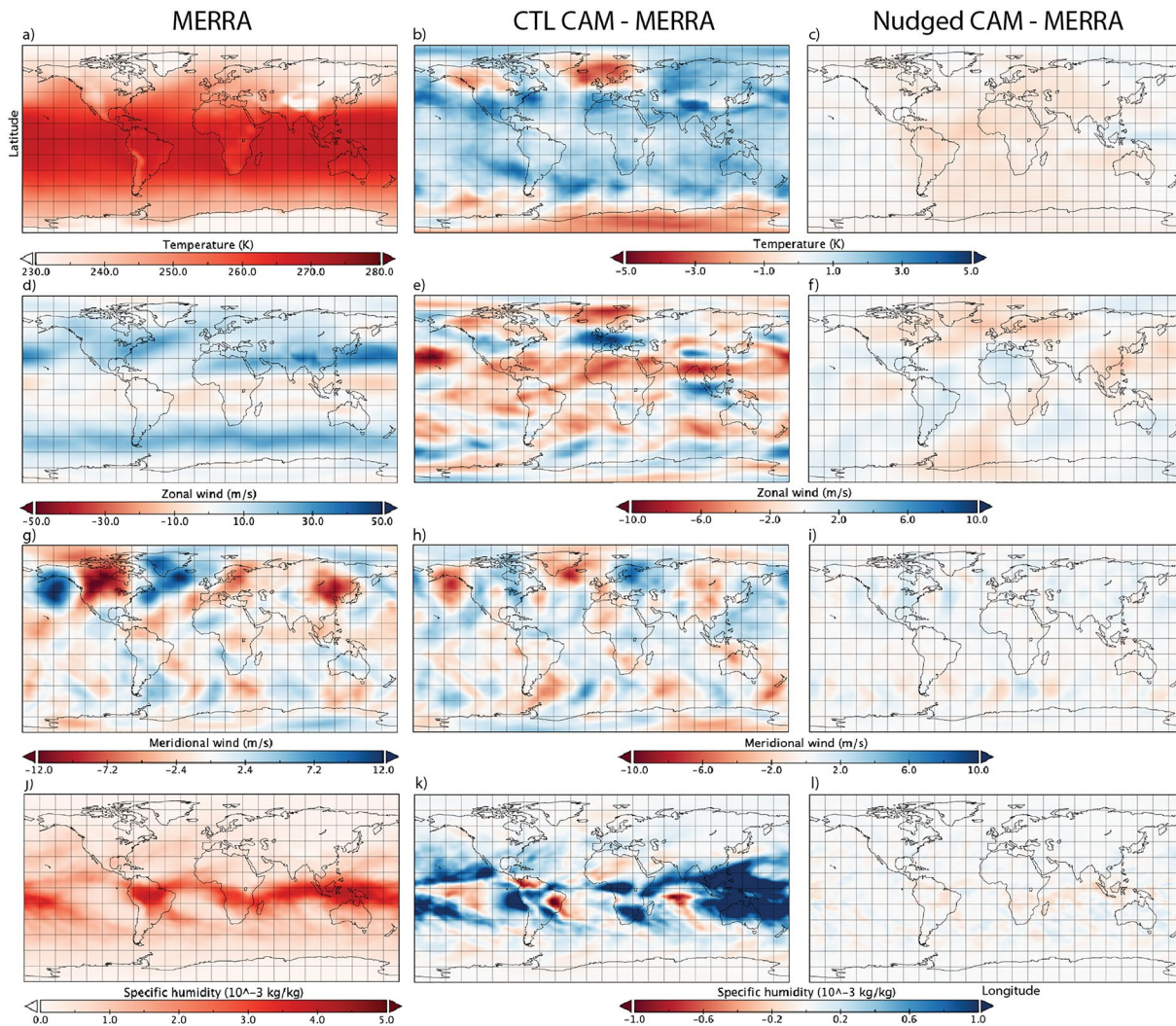


Figure 3. The temperature mean state of Modern Era Retrospective-Analysis for Research and Applications, Version 2 (MERRA) in January at 500 hPa (a), the difference between the control Community Atmosphere Model (CAM) and MERRA (b), and the difference between the nudged CAM and MERRA (c). As in (a) to (c) but for zonal wind (d)–(f), meridional wind (g)–(i), and specific humidity (j)–(l).

At 500 hPa, Figure 3 shows that the control run has a large patch of negative temperature mean bias over the North Sea, which is particularly pronounced relative to the positive temperature mean bias that covers most of the Northern Hemisphere. In the nudged CAM, this patch disappears, replaced with weaker and more diffuse negative temperature mean bias across most of the globe. The zonal wind mean bias in the control run has strong bands of mean bias across the midlatitudes; in the nudged run the mean bias is once again much weaker and more diffuse. Of particular note is the correction to jet strength over Northern Europe, where CAM tends to favor the Central and Southern positions of the jet (Hannachi et al., 2012) to the exclusion of the Northern position, a mean bias which is corrected in the nudged run. Mean biases in meridional wind look similar between the control and nudged runs, although substantially reduced in magnitude in the latter. The moisture mean bias in the control run is strongest by far in the equatorial regions, and is largely corrected in the nudged run.

The blocking frequency patterns are also improved substantially in the nudged ensemble, particularly in the Euro-Atlantic sector (Figure 4). The root mean square error in blocking frequency is 0.015 between the control run and MERRA, which improves to 0.011 for the nudged CAM.

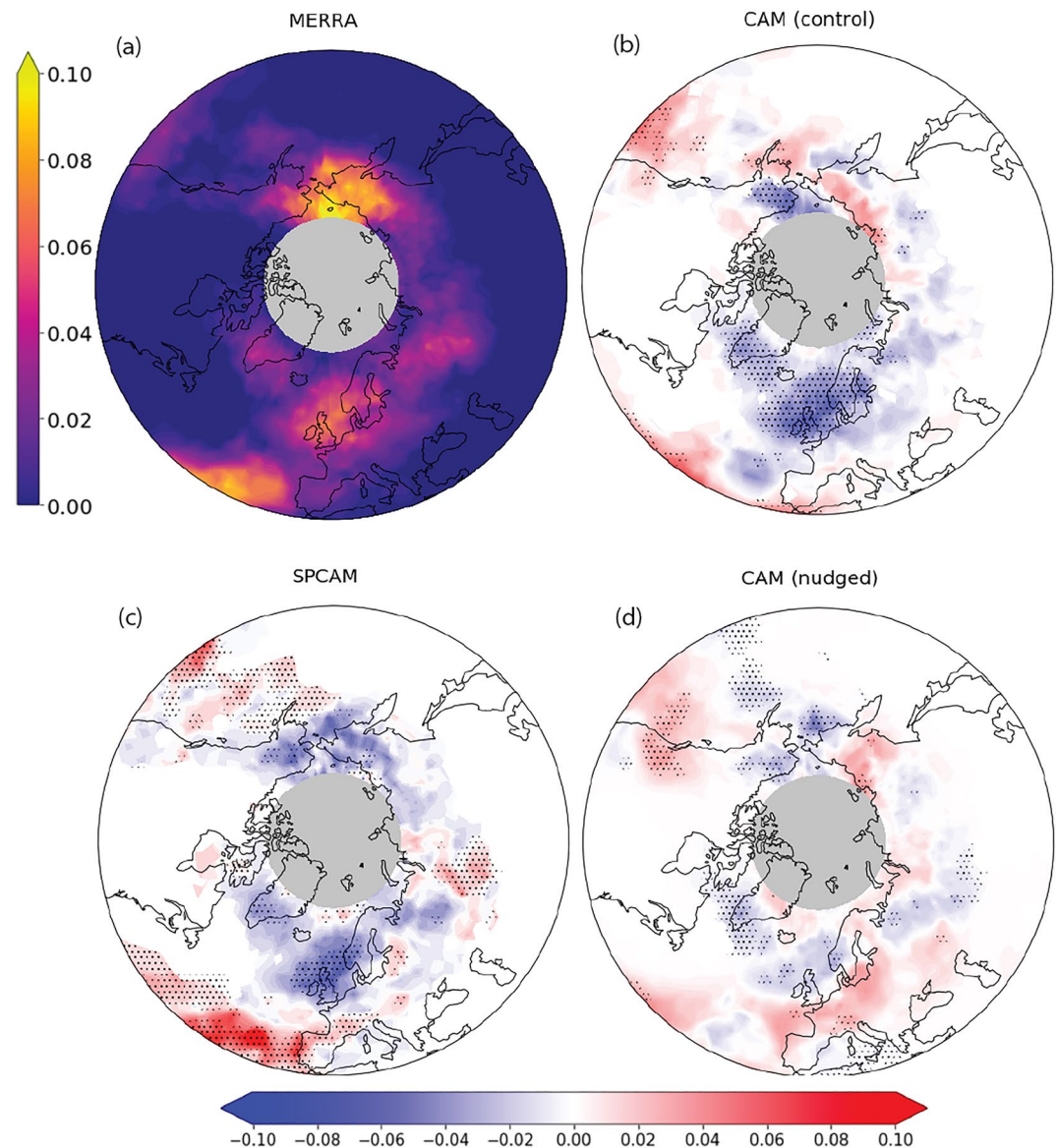


Figure 4. Fraction of January days blocked according to the Scherrer et al. (2006) index in (a) interpolated Modern Era Retrospective-Analysis for Research and Applications, Version 2 (MERRA) data from 1980 to 2017. Difference in fraction of January days blocked between MERRA data and (b) 40-year control run of CAM (c) 20-year run of SPCAM and (d) a 38-member ensemble of CAM after nudging has been applied. Stippling indicates the area where the difference is significant.

3.3. Local Wave Activity Index

When applied to our data, the Martineau et al. (2017) index gives similar results to the Scherrer et al. (2006) index, with SPCAM and the control CAM underestimating blocking over Europe, while the nudged CAM has a blocking frequency quite close to MERRA, especially over Europe (Figure 5). In fact, the RMSE for the Martineau et al. (2017) index improves from 0.035 between the control run and MERRA to 0.018 between the nudged run and MERRA.

3.4. Anomaly Index

The anomaly index gives results that were more equivocal than the other two indices. If we use a fixed anomaly threshold of 250 m, we get a similar overall RMSE for the nudged CAM and SPCAM—both have an

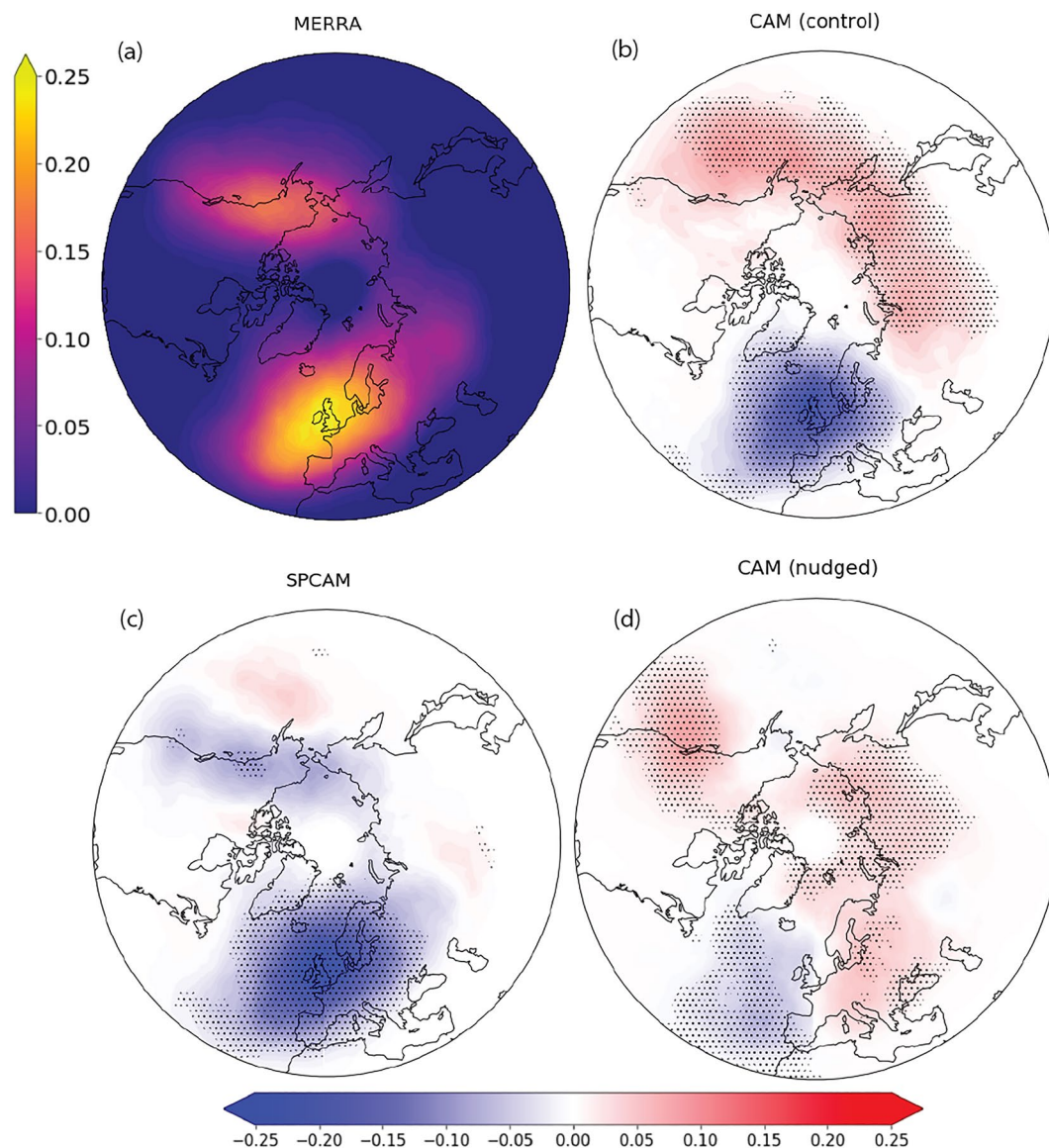


Figure 5. Fraction of January days blocked according to the Martineau et al. (2017) index in (a) interpolated Modern Era Retrospective-Analysis for Research and Applications, Version 2 (MERRA) data from 1980 to 2017. Difference in fraction of January days blocked between MERRA data and (b) 40-year control run of CAM (c) 20-year run of SPCAM and (d) a 38-member ensemble of CAM after nudging has been applied. Stippling indicates the area where the difference is significant.

RMSE versus MERRA of 0.018, compared to 0.021 for the control CAM—although the error in the nudged CAM is more contained in the higher mean blocking frequency across the Northern Hemisphere rather than in deviations from that mean (Figure S1). This seems to be largely due to the fact that the standard deviation in geopotential height (across the entire region 35°N–75°N.) is larger for the nudged CAM (253 m) than it is for MERRA (227 m), the control CAM (242 m) or SPCAM (233 m), for reasons that we do not entirely understand. When we correct for this difference by changing from a fixed anomaly threshold to one that is equal to the standard deviation of a given simulation (Figure S2), the nudged CAM has a lower RMSE versus MERRA of 0.014, while SPCAM and control CAM remain largely unchanged with RMSE of 0.020 and 0.022, respectively.

4. Conclusions

When the mean state bias in CAM is reduced, the blocking underestimation improves dramatically. This change is not seen when we switch to a model version that better captures convection, suggesting that the model's difficulty in accurately reproducing blocking patterns stems from problems with its mean state and that reductions in blocking underestimation are best achieved by improving the model mean state overall. This process will likely include changes to the model physics (Williams et al., 2020), but our results indicate that the focus should be on making those changes that best improve the mean state rather than improving physical processes that are perceived as more directly related to blocking.

Further work is necessary to determine if this pattern holds true for other climate models, most of which have also been found to underestimate blocking at least in part as a result of mean state bias (Anstey et al., 2013; Vial & Osborn, 2012).

Data Availability Statement

Data displayed in this paper are available at <https://dataverse.harvard.edu/dataset.xhtml?persistentId=doi:10.7910/DVN/1QDGT>.

Acknowledgments

This research was supported by NASA grant 80NSSC17K0267 and NSF grant AGS-1552385. The computations in this paper were run on the Odyssey cluster supported by the FAS Division of Science, Research Computing Group, at Harvard University.

References

- Anstey, J. A., Davini, P., Gray, L. J., Woollings, T. J., Butchart, N., Cagnazzo, C., et al. (2013). Multi-model analysis of northern hemisphere winter blocking: Model biases and the role of resolution. *Journal of Geophysical Research: Atmospheres*, 118(10), 3956–3971. <https://doi.org/10.1002/jgrd.50231>
- Bellucci, A., Gualdi, S., & Navarra, A. (2010). The double-ITCZ syndrome in coupled general circulation models: The role of large-scale vertical circulation regimes. *Journal of Climate*, 23(5), 1127–1145. <https://doi.org/10.1175/2009JCLI3002.1>
- Berckmans, J., Woollings, T., Demory, M.-E., Vidale, P.-L., & Roberts, M. (2013). Atmospheric blocking in a high resolution climate model: Influences of mean state, orography and eddy forcing. *Atmospheric Science Letters*, 14(1), 34–40. <https://doi.org/10.1002/asl2.412>
- Chan, P.-W., Hassanzadeh, P., & Kuang, Z. (2019). Evaluating indices of blocking anticyclones in terms of their linear relations with surface hot extremes. *Geophysical Research Letters*, 46(9), 4904–4912. <https://doi.org/10.1029/2019gl083307>
- Francis, J. A., & Vavrus, S. J. (2012). Evidence linking arctic amplification to extreme weather in mid-latitudes. *Geophysical Research Letters*, 39(6). <https://doi.org/10.1029/2012gl051000>
- Gelaro, R., McCarty, W., Suárez, M. J., Todling, R., Molod, A., Takacs, L., et al. (2017). The Modern-Era Retrospective Analysis for Research and Applications, Version 2 (MERRA-2). *Journal of Climate*, 30(14), 5419–5454. <https://doi.org/10.1175/JCLI-D-16-0758.1>
- Hannachi, A., Woollings, T., & Fraedrich, K. (2012). The North Atlantic jet stream: A look at preferred positions, paths and transitions. *Quarterly Journal of the Royal Meteorological Society*, 138(665), 862–877. <https://doi.org/10.1002/qj.959>
- Kennedy, D., Parker, T., Woollings, T., Harvey, B., & Shaffrey, L. (2016). The response of high-impact blocking weather systems to climate change. *Geophysical Research Letters*, 43(13), 7250–7258. <https://doi.org/10.1002/2016gl069725>
- Khairoutdinov, M., Randall, D., & DeMott, C. (2005). Simulations of the atmospheric general circulation using a cloud-resolving model as a superparameterization of physical processes. *Journal of the Atmospheric Sciences*, 62(7), 2136–2154. <https://doi.org/10.1175/JAS3453.1>
- Ma, D., & Kuang, Z. (2016). A mechanism-denial study on the madden-julian oscillation with reduced interference from mean state changes. *Geophysical Research Letters*, 43(6), 2989–2997. <https://doi.org/10.1002/2016gl067702>
- Maloney, E. D., & Hartmann, D. L. (2001). The sensitivity of intraseasonal variability in the NCAR CCM3 to changes in convective parameterization. *Journal of Climate*, 14(9), 2015–2034. [https://doi.org/10.1175/1520-0442\(2001\)014<2015:TSOIVI>2.0.CO;2](https://doi.org/10.1175/1520-0442(2001)014<2015:TSOIVI>2.0.CO;2)
- Martineau, P., Chen, G., & Burrows, D. A. (2017). Wave events: Climatology, trends, and relationship to Northern Hemisphere winter blocking and weather extremes. *Journal of Climate*, 30(15), 5675–5697. <https://doi.org/10.1175/JCLI-D-16-0692.1>
- Masato, G., Hoskins, B. J., & Woollings, T. (2013). Winter and summer northern hemisphere blocking in cimp5 models. *Journal of Climate*, 26(18), 7044–7059. <https://doi.org/10.1175/JCLI-D-12-00466.1>
- Masato, G., Hoskins, B. J., & Woollings, T. J. (2009). Can the frequency of blocking be described by a red noise process? *Journal of the Atmospheric Sciences*, 66(7), 2143–2149. <https://doi.org/10.1175/2008JAS2907.1>
- Nakamura, N., & Huang, C. S. Y. (2018). Atmospheric blocking as a traffic jam in the jet stream. *Science*, 361(6397), 42–47. <https://doi.org/10.1126/science.aat0721>
- Pfahl, S., Schwierz, C., Croci-Maspoli, M., Grams, C. M., & Wernli, H. (2015). Importance of latent heat release in ascending air streams for atmospheric blocking. *Nature Geoscience*, 8(8), 610–614. <https://doi.org/10.1038/ngeo2487>
- Pfahl, S., & Wernli, H. (2012). Quantifying the relevance of atmospheric blocking for co-located temperature extremes in the northern hemisphere on (sub-) daily time scales. *Geophysical Research Letters*, 39(12). <https://doi.org/10.1029/2012gl052261>
- Rex, D. F. (1950). Blocking action in the middle troposphere and its effect upon regional climate. *Tellus*, 2(3), 196–211. <https://doi.org/10.1111/j.2153-3490.1950.tb00331.x>
- Scaife, A. A., Copsey, D., Gordon, C., Harris, C., Hinton, T., Keeley, S., et al. (2011). Improved Atlantic winter blocking in a climate model. *Geophysical Research Letters*, 38(23). <https://doi.org/10.1029/2011GL049573>
- Scherrer, S. C., Croci-Maspoli, M., Schwierz, C., & Appenzeller, C. (2006). Two-dimensional indices of atmospheric blocking and their statistical relationship with winter climate patterns in the euro-atlantic region. *International Journal of Climatology*, 26(2), 233–249. <https://doi.org/10.1002/joc.1250>
- Schiemann, R., Demory, M.-E., Shaffrey, L. C., Strachan, J., Vidale, P. L., Mizielinski, M. S., et al. (2017). The resolution sensitivity of northern hemisphere blocking in four 25-km atmospheric global circulation models. *Journal of Climate*, 30(1), 337–358. <https://doi.org/10.1175/JCLI-D-16-0100.1>

- Shutts, G. J. (1983). The propagation of eddies in diffluent jetstreams: Eddy vorticity forcing of 'blocking' flow fields. *Quarterly Journal of the Royal Meteorological Society*, 109(462), 737–761. <https://doi.org/10.1002/qj.49710946204>
- Simpson, I. R., Bacmeister, J., Neale, R. B., Hannay, C., Gettelman, A., Garcia, R. R., et al. (2020). An evaluation of the large-scale atmospheric circulation and its variability in cesm2 and other cmip models. *Journal of Geophysical Research: Atmospheres*, 125(13), e2020JD032835. <https://doi.org/10.1029/2020JD032835>
- Steinfeld, D., & Pfahl, S. (2019). The role of latent heating in atmospheric blocking dynamics: A global climatology. *Climate Dynamics*, 53(9–10), 6159–6180. <https://doi.org/10.1007/s00382-019-04919-6>
- Tibaldi, S., & Molteni, F. (1990). On the operational predictability of blocking. *Tellus*, 42(3), 343–365. <https://doi.org/10.1034/j.1600-0870.1990.t01-2-00003.x>
- Tyrlis, E., & Hoskins, B. J. (2008). Aspects of a northern hemisphere atmospheric blocking climatology. *Journal of the Atmospheric Sciences*, 65(5), 1638–1652. <https://doi.org/10.1175/2007JAS2337.1>
- Vial, J., & Osborn, T. J. (2012). Assessment of atmosphere-ocean general circulation model simulations of winter northern hemisphere atmospheric blocking. *Climate Dynamics*, 39(1–2), 95–112. <https://doi.org/10.1007/s00382-011-1177-z>
- Wang, Y., Zhang, G. J., & Craig, G. C. (2016). Stochastic convective parameterization improving the simulation of tropical precipitation variability in the ncar cam5. *Geophysical Research Letters*, 43(12), 6612–6619. <https://doi.org/10.1002/2016gl069818>
- Williams, K. D., van Niekerk, A., Best, M. J., Lock, A. P., Brooke, J. K., Carvalho, M. J., et al. (2020). Addressing the causes of large-scale circulation error in the met office unified model. *Quarterly Journal of the Royal Meteorological Society*, 146(731), 2597–2613. <https://doi.org/10.1002/qj.3807>
- Woollings, T., Barriopedro, D., Methven, J., Son, S.-W., Martius, O., Harvey, B., et al. (2018). Blocking and its response to climate change. *Current Climate Change Reports*, 4, 1–300. <https://doi.org/10.1007/s40641-018-0108-z>
- Yamazaki, A., & Itoh, H. (2009). Selective absorption mechanism for the maintenance of blocking. *Geophysical Research Letters*, 36(5). <https://doi.org/10.1029/2008gl036770>